Predicting desaturation by biogenic gas formation via denitrification during centrifugal loading

C.A. Hall, L.A. van Paassen, B. E. Rittmann, & E. Kavazanjian Jr.
School of Sustainable Engineering and the Built Environment, Arizona State University, Tempe, AZ, USA
J.T. DeJong & D.W. Wilson
Department of Civil and Environmental Engineering, University of California, Davis, Davis, CA, USA

ABSTRACT: Microbially induced desaturation and precipitation (MIDP) via denitrification has the potential to reduce earthquake-induced liquefaction potential by two mechanisms: calcium carbonate precipitation to mechanically strengthen soil and biogenic gas production to desaturate and dampen pore pressure changes in soil. Lab-scale tests have demonstrated effective desaturation and improved mechanical strength by MIDP. However, in laboratory tests, gas pockets and lenses form causing upheaval as a result of low overburden pressures. The characteristics of biogenic gas formation, distribution, and retention need to be evaluated to gain comprehensive understanding of the effectiveness of this treatment at depth before and after an earthquake event. MIDP treatment during centrifuge loading conditions is being performed to simulate field stress conditions, prior to complete process scale-up for field application. A simplified numerical model was developed to evaluate the scaling effects on biogenic gas generation between the centrifuge model and prototype scale. The results indicate that diffusion of soluble N_2 is negligible at both the model and prototype scales for the simulated reaction rate. However, the simplified model did not consider other pore-scale influences and mixing from liquid-gas transfer and transport. Future modeling work will need to add these features.

1 INTRODUCTION

Saturated, cohesionless soils are at risk of liquefying due to earthquake events that may lead to significant infrastructure damage. The primary mechanism leading to earthquake-induced liquefaction is the build-up of excess pore water pressure resulting from seismic loading, which reduces the effective stress (Vaid and Sivathayalan 2000). Biologically driven ground improvement through microbially induced carbonate precipitation by urea hydrolyzing bacteria has been proposed and shown to successfully improve the soil's mechanical properties at lab- and field-scale (DeJong et al. 2010; van Paassen et al. 2010). However, the process is still costly and resulting by-products from this process are potentially harmful.

An alternative bio-based solution to reduce liquefaction triggering is microbially induced desaturation and precipitation (MIDP) by dissimilatory nitrate reduction, or denitrification. This results in calcium carbonate precipitation and biogenic di-nitrogen gas (N_2) production that has the potential to reduce liquefaction triggering by mechanically strengthening and decreasing the ratio of water volume to voids volume, or the degree of saturation, of the soil, respectively (O'Donnell 2017a; Pham 2017; van Paassen et al. 2010). As biocementation by denitrification can be time intensive, interest in biogenic gas production has increased due to its potential to dampen pore pressure rise during seismic loading by increasing the compressibility of the pore space, thereby reducing the potential for liquefaction triggering (He et al. 2011; O'Donnell 2017a; O'Donnell 2017b; Pham et al. 2017; Rebata-Landa and Santamarina 2012).

For liquefaction mitigation, the primary biogenic gas of interest generated by denitrification is N_2, as it has a relatively low solubility and is the most abundantly produced biogenic gas compared to other gas by-products (e.g., CO_2). Lab experiments have shown that even minimal desaturation by N_2 can significantly increase the undrained shear strength and liquefaction resistance of the soil (He and Chu 2013; Rebata-Landa and Santamarina 2012). However, due to the low pressure of most lab-scale specimens, the gas pressure produced by the microbial metabolism may exceed the overburden pressure. This can result in formation of gas pockets or gas lenses, as shown in Figure 1.

We performed physical modelling experiments in a centrifuge at a gravitation acceleration of 80 *g* to improve current knowledge regarding the production,

migration, and retention of biogenic gas and to provide insight about the behavior and treatment effectiveness before and after an earthquake event at depths beyond the lab scale. We used a simplified numerical model to evaluate the scaling effects between the centrifuge model and prototype at field scale and to predict and interpret the centrifuge model results. Detailed herein is the numerical modelling approach developed to predict biogenic gas behavior and characteristics in the model and prototype environment.

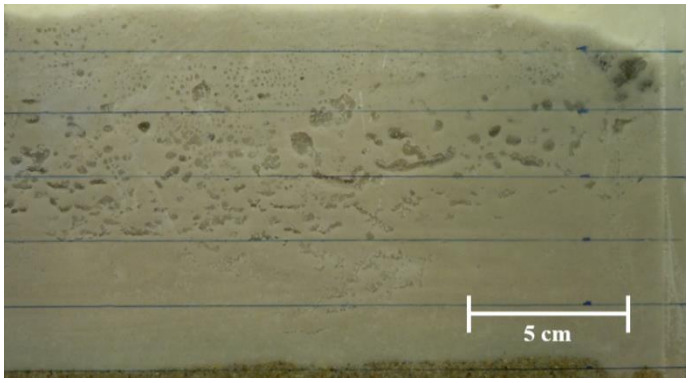

Figure 1. Biogenic gas pockets in 1 *g* experiment, 10 days after MIDP via denitrification treatment.

2 SIMPLIFIED MODEL TO PREDICT THE VOLUME OF BIOGENIC GAS UNDER CENTRIFUGAL LOADING

2.1 *Achieving initial target degree of gas saturation*

In the simplified numerical model, N_2 was the only gas considered. While CO_2 also is a by-product of denitrification and biomass decay, it was assumed that any desaturation resulting from CO_2 would be negligible due to the high solubility of CO_2 at prototype depth. It also was assumed that the soil profile was a closed system and NO_3^- (provided as substrate) undergoes complete reduction to N_2. The effects of vapor barriers at the inter-particle soil contacts were neglected. Based on methods provided by Pham (2017), Eq. 1 estimates the required concentration of consumed NO_3^- ($[NO_3^-]_{con}$, mol m^{-3}) by microbes to achieve desired gas volume (V_g) in the total pore volume (V_P) which is defined as the degree of gas saturation (S_g, dimensionless) at 1 *g*.

$$[NO_3^-]_{con} = \frac{Y_{NO_3^-} P_{N2,m}}{Y_{N_2}} \left(\frac{S_g}{RT} + k_{H,N2}\right) \quad (1)$$

where Y_{N2} and Y_{NO3-} are the stoichiometric coefficients of N_2 and NO_3^- during denitrification, respectively, $P_{N2,m}$ (atm) is the partial pressure of the model and is assumed to be equal to the hydraulic pressure in the saturated soil environment, T (K) is the system temperature, R (atm L K^{-1} mol^{-1}) is the universal gas constant, and $k_{H,N2}$ is Henry's constant for N_2 at standard temperature (mol L^{-1} atm^{-1}). It was assumed that the initial soil condition is fully water saturated at $P_{N2,m}$, which is equal to the hydrostatic pressure that is a function of specific weight of water (γ_w, kN m^{-3}) and the depth below the phreatic surface of the model.

As treatment is introduced at 1 *g* and ambient pressure, the desaturation capacity is limited by what can be achieved at 1 atm and does not vary significantly across the shallow depth of the test set-up. The volumetric at the gas percolation threshold at ambient temperature and pressure was shown to be approximately 80% given experimental sand grain size and over burden considerations (Pham, 2017). Maximum microbial metabolism was assumed to have Y_{NO3} and Y_{N2} stoichiometric coefficient values of 0.97 and 0.39, respectively. Therefore, considering maximum microbial metabolism stoichiometry to theoretically reduce the degree of saturation by 20%, the required $[NO_3^-]_{con}$ was estimated to be 22 mol m^{-3} at 1 atm.

2.2 *Modelling gas production and distribution in the centrifuge*

Eq. 2 was used to estimate the production rate of N_2 gas in the pore space (r_{N2}, mol m^{-3} h^{-1}) via single-step denitrification according to Monod kinetics,

$$r_{N2} = 0.5 q_S C_X \left(\frac{C_{NO3}}{K_{NO3} + C_{NO3}}\right) V_P \quad (2)$$

where 0.5 is the stoichiometric ratio of N for NO_3^- and N_2 gas, q_S (mol g^{-1} of biomass h^{-1}) is the maximum substrate utilization rate, C_X (g biomass m^{-3}) is the amount of active biomass, C_{NO3} (mol m^{-3}) is the concentration of NO_3^-, K_{NO3} (mol m^{-3}) is the half-saturation constant for the substrate, and V_P (m^3) is the pore volume. q_S is defined by Eq. 3 as

$$q_S = \mu_{max} Y_{SX} \quad (3)$$

where μ_{max} (h^{-1}) is the maximum theoretical microbial growth rate and Y_{SX} (dimensionless) is the stoichiometric ratio of nitrate in the substrate to biomass production considering all microbial metabolisms for maximum growth. V_P was estimated using Eq. 4, given a known soil relative density.

$$V_P = \left(\frac{V_T(e_{max} - D_R(e_{max} - e_{min}))}{1 + e_{max} - D_R(e_{max} - e_{min})}\right) \quad (4)$$

where V_T (m^3) is the total volume, e_{max} (dimensionless) is the soil void ratio in its loosest state, D_R (g m^{-3}) is the relative soil density, and e_{min} (dimensionless) is the soil void ratio in its densest state.

The rate at which nitrogen gas is produced is a function of the microbial metabolism and the concentration of active biomass (C_x). Substrate limitations

also influence the rate of N_2 production. As such, assuming initial NO_3^- concentrations of 22 mol m^{-3} and K_{NO3} to be 0.36 mol NO_3^- m^{-3} (Pham 2017) based on the observed nitrate consumption the resulting initial r_{N2} is assumed to be 0.085 mol N_2 h^{-1}. This rate changes as substrate is consumed and biomass accumulates. However, for this simplified model, biomass was assumed to be constant.

Based on the pressure-scaling laws under centrifugal loading, the prototype hydrostatic pressure ($P_{N2,P}$, atm) and the depth scale are linearly related by the gravity acceleration factor induced on the soil in the model, g (Garnier et al. 2007; Caicedo and Thorel 2014; Kutter 1992). The pressure increase upon loading directly influences gas solubility, and the resulting estimated amount of $N_{2,(g)}$ in the gas phase is given by Eq. 5.

$$N_{2(g),P} = \frac{\left(r_{N2}\ t - c_{N_{2(aq)}}\right)RT}{P_{N_2,P}} \quad (5)$$

where t (h^{-1}) is the reaction duration, and $c_{N2(aq)}$ (mol m^{-3}) is the concentration of aqueous $N_{2,(g)}$ gas in equilibrium as determined by Henry's law, and $P_{N2,P}$ (atm) is the simulated pressure of the prototype environment and is assumed to be the hydrostatic pressure of the pore fluid. Since relative density and grain size influence the total available space for gas to form and the volume of initial pore fluid, the pore volume should be considered for desaturation.

It was assumed that the soil particles were spatially fixed and homogenously sized. For the results described here, sand (D_{50} = 0.2 mm) at 40% relative density was used, resulting in Vp values of 0.41 m^3 per m^3 of soil. Additionally, it was assumed that initial pore fluid composition was well-mixed and uniform throughout the soil, but was subject to diffusive transport and phase transfer beyond t = 0.

One of the limitations of centrifuge testing is that the reaction rate, r_{N2}, and diffusive transport are considered not to be influenced by centrifuge spinning, unlike stress and pressure. The diffusion time in the model is scaled by the squared gravitational constant, g^{-2}, compared with the diffusion time in the prototype (Kutter 1992). Consequently, diffusive fluxes are expected to be greater in the model than for the prototype. This leads to the question of whether the gas distribution in the model would be representative of the gas distribution in the prototype or whether the gas distribution would be different as a result of the increased diffusive flux in the model.

The equation for diffusion in the prototype at depth node i ($J_{P,i}$, mol m^{-1} h^{-1}) is detailed in Eq. 6.

$$J_{P,i} = -D_{N2,aq}\ \frac{\partial c_{N2}}{\partial x_P} \quad (6)$$

where $D_{N2,aq}$ (mol m^{-2} h^{-1}) is the diffusion coefficient of aqueous $N_{2,(aq)}$ and x_P (m) is the distance in the prototype, respectively. The equation for diffusion at the model scale is defined in Eq. 7.

$$J_{m,i} = -D_{N2,aq} g^2\ \frac{\partial c_{N2}}{\partial x_m} \quad (7)$$

where x_m (m) is the distance in the model.

To consider diffusive flux between the soil layers, neglecting additional kinetic and friction factors from travelling through porous media, $D_{N2,aq}$ was assumed to be 7.2E-6 m^2 h^{-1} at 298 K and independent of pressure effects, as reported by Cadogan et al. (2014).

A flux balance equation considering aqueous $N_{2,(aq)}$ diffusion between the soil layers, gaseous $N_{2,(g)}$ formation, and the production rate was used to estimate the aqueous $N_{2,(g)}$ gas concentration at simulated prototype depth. Eq. 8 details the aqueous $N_{2,(aq)}$ concentration flux at a given i and t.

$$\frac{dN_{2(aq),P}}{dt} = r_{N2}\ - c_{N_{2(g)}} + J_{P,i-1} - J_{P,i} \quad (8)$$

where $c_{N2(g)}$ (mol m^{-3}) is the concentration of N_2 transitioning from the liquid to the gas phase assuming equilibrium and $J_{P,i}$ (mol m^{-1} h^{-1}) is the diffusion from i at the prototype scale. Since equilibrium is assumed, the transition of N_2 from the liquid to the gas phase is instantaneous. As a result, $c_{N2(g)}$ is based on the previously accumulated $N_{2(aq),P}$ at t-1 and r_{N2} at t.

To identify the significance of diffusion on the concentration of soluble $N_{2,(aq)}$, the second Damköhler number, which relates the rate of complete denitrification and diffusion, is determined for the prototype ($Da_{II,P}$) and model scale ($Da_{II,m}$) in Eq. 9 and 10, respectively (Connolly et al., 2015).

$$Da_{II,P} = \frac{r_{N2}}{J_{P,i}} \quad (9)$$

$$Da_{II,m} = \frac{r_{N2}}{J_{m,i}} \quad (10)$$

3 SIMPLIFIED MODEL RESULTS AND DISCUSSION

Figure 2 illustrates the concentration of aqueous N_2 for prototype and model scale conditions, considering aqueous $N_{2,(aq)}$ diffusion between the soil layers, gaseous $N_{2,(g)}$ formation at a constant production rate from microbial nitrate reduction, equilibrium, and no advective flux of biogenic gas.

Soluble $N_{2(aq)}$ saturation is achieved at upper levels shortly after 6 hours at both scales. After 12 hours, equilibrium is reached over the total depth in both scales and all additional produced biogenic N_2 enters

the gas phase. There is notably little difference between the prototype or model conditions on soluble $N_{2,(aq)}$ concentration during the modelled time-period, which implies that the dominating mechanisms scale linearly under centrifuge loading.

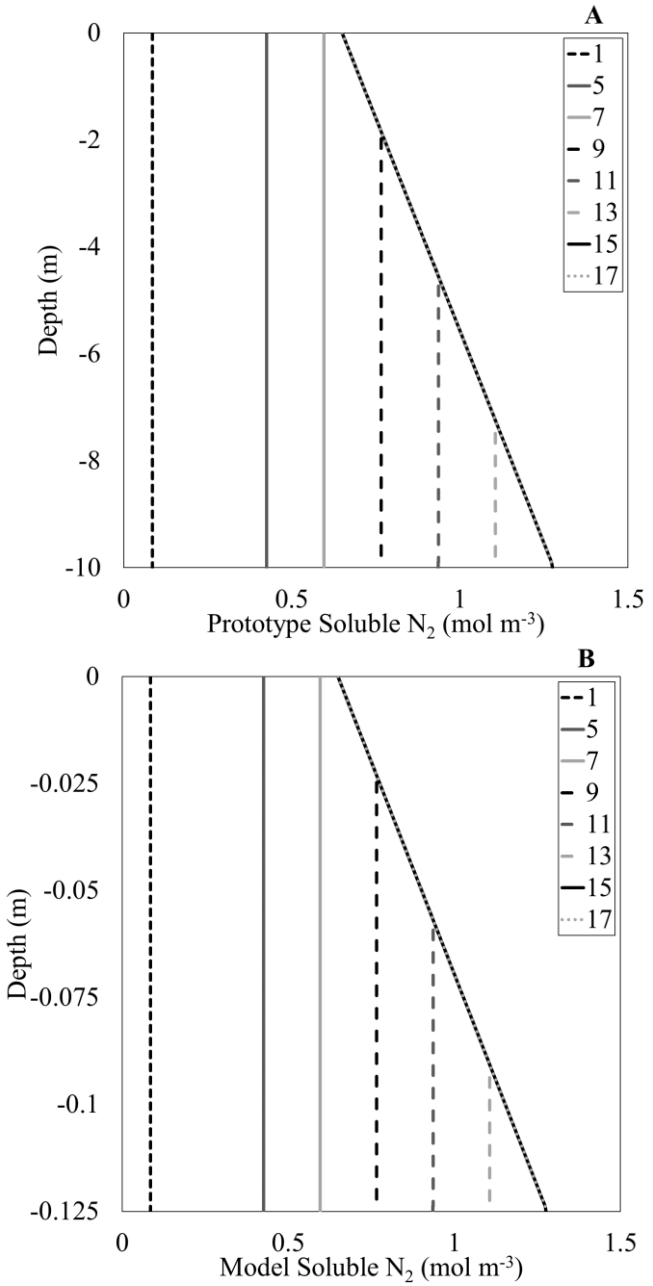

Figure 2. Soluble N_2 ($c_{N2(aq)}$) at equilibrium considering biogenic N_2 production (r_{N2}), aqueous $N_{2,(aq)}$ diffusion between the layers ($J_{P,i}$ and $J_{P,i-1}$), and liquid-gas transfer ($c_{N2(g)}$) in Ottawa F-65 sand at 40% relative density at [A] simulated prototype and [B] model scale conditions from t = 1 to 17 hours.

Once liquid-gas phase equilibrium is reached, the soluble $N_{2,(aq)}$ concentration gradient varies linearly with depth. Figure 3 shows the diffusive flux from the lower level, *i-1* to the upper level, *i,* ($J_{P,i-1}$). As the reaction rate is constant over depth, diffusion is zero until shortly after 6 hours, when the liquid-gas phase threshold was met at the surface. After that, diffusive flux changes step-wise over time in both scales and as the solubility changes linearly with depth, saturation is achieved at increasing depths as a linear function of time. Since diffusion scales by g^2, unlike pressure and stress which scale linearly, this results in much faster diffusion in the model than at the prototype scale.

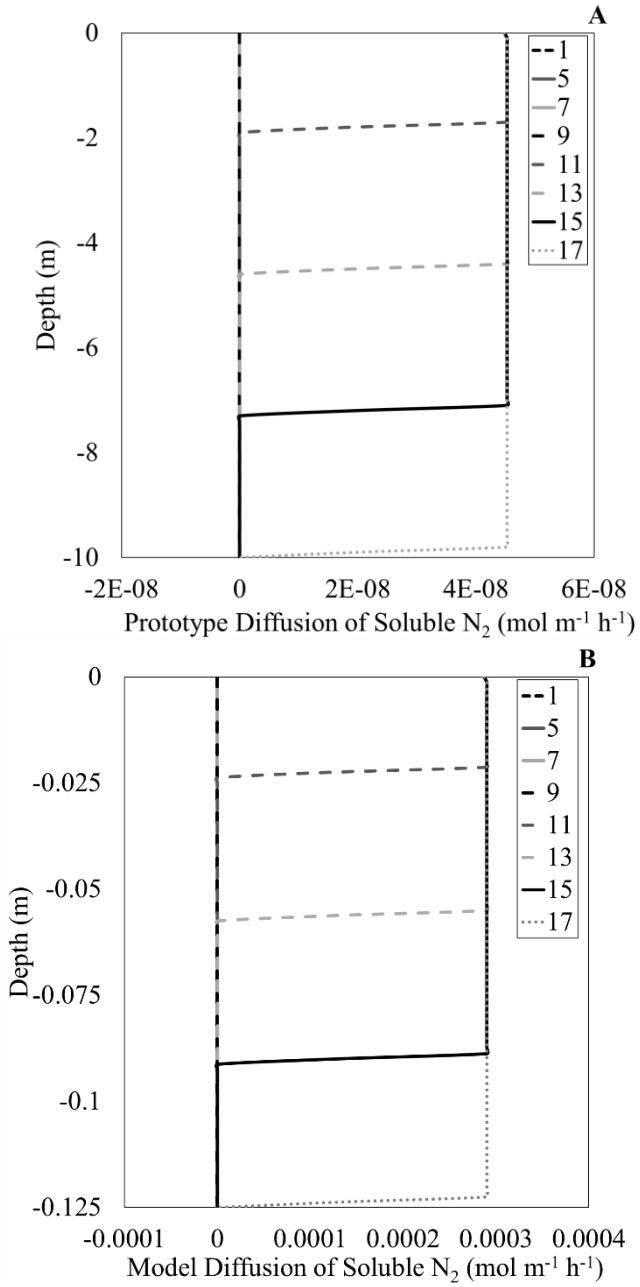

Figure 3. Diffusion rate of liquid-phase $N_{2,(aq)}$ ($J_{P,i-1}$) going into each discretized layer in Ottawa F-65 sand at 40% relative density at [A] simulated prototype and [B] model scale conditions from t = 1 to 17 hours.

For the cases illustrated in Figures 2 and 3, $Da_{(II),P}$ and $Da_{(II),m}$ were calculated at 2,363,967 and 369, respectively. As the Damköhler numbers for either scale was greater than 10, it can be considered that diffusion rate is insignificant compared to the reaction rate and it can be assumed that the substrate is immediately converted (Folger 2005). Therefore, it was concluded that diffusion did not have a significant effect

during this time-period. However, in reality the second Damköhler number may decrease as the reaction rate decreases, for example when substrates are getting depleted or due to inhibition of intermediate nitrogen compounds. Substrate limitation may also occur when the saturation drops and some of the denitrifying bacteria lose contact with the liquid phase or due to diffusion limitations at the pore scale.

In the current model, the diffusive fluxes in and out of each layer are equal, except for the bottom and the top layer, resulting in a relatively constant diffusion over the domain between layers and a net diffusion balance of approximately zero. As a consequence, the transfer of N_2 from the solute phase to the gas phase in each layer is unaffected by the diffusive flux and once the liquid-gas equilibrium concentration is reached, the transfer of N_2 from the solute phase to the gas phase is equal to the reaction rate.

The accumulated $N_{2,(g)}$ gas content in the prototype considering soluble $N_{2,(aq)}$ production, diffusion, and phase equilibrium is shown in Figure 4. It was assumed that gas produced at varying depths over time was fixed, evenly horizontally distributed, and did not diffuse through the soil. Figure 4 illustrates the overall gas volume at each layer, assuming pore-level and distribution effects are negligible.

Figure 4 shows that the upper layers of sand experience much lower degree of saturation, though the concentration of gas is linearly distributed. This makes sense considering the volume of the gas, calculated using the ideal gas law, is proportional to the pressure. As a further result of a changing profile in the degree of saturation over the depth, the hydraulic conductivity of the upper layers of soil is expected to be less than soil at depth.

Although the model seems to indicate that diffusion is not significantly influencing the gas distribution and resulting development of gas saturation in time, other pore-scale influences and mixing from liquid-gas transfer and transport were not considered in this simplified model. These other factors may influence the gas and aqueous N_2 concentrations, the gas distribution at the pore scale, and ultimately the resulting degree of saturation. Future modeling efforts should consider gas bubble nucleation, diffusive fluxes at pore scale, and capillary pressure in the gas phase. Enhancements to understanding the pressure differences to resolve the differences between the model and prototype scale will allow for the use of saturation-based Richard's equation. Additionally, modeling advective transport of the gas phase, which may occur when the bubbles are smaller than the pore throats or when the capillary pressure of the gas phase exceeds the air entry value of the pore throats, will improve the ability to predict the distribution and migration of the gas, the potential formation of gas pockets, and the escape of the gas to the atmosphere. These improvements will enhance interpretation of the physical model results and provide insight on the potential future challenges when applying MIDP via denitrification to mitigate liquefaction risk at the field-scale. Soil characteristics, like permeability and suction, resulting from biogenic gas production are influenced by the distribution and movement of gas pre- and post-liquefaction and will likely need to be evaluated on a case-by-case basis as soil type and structure changes.

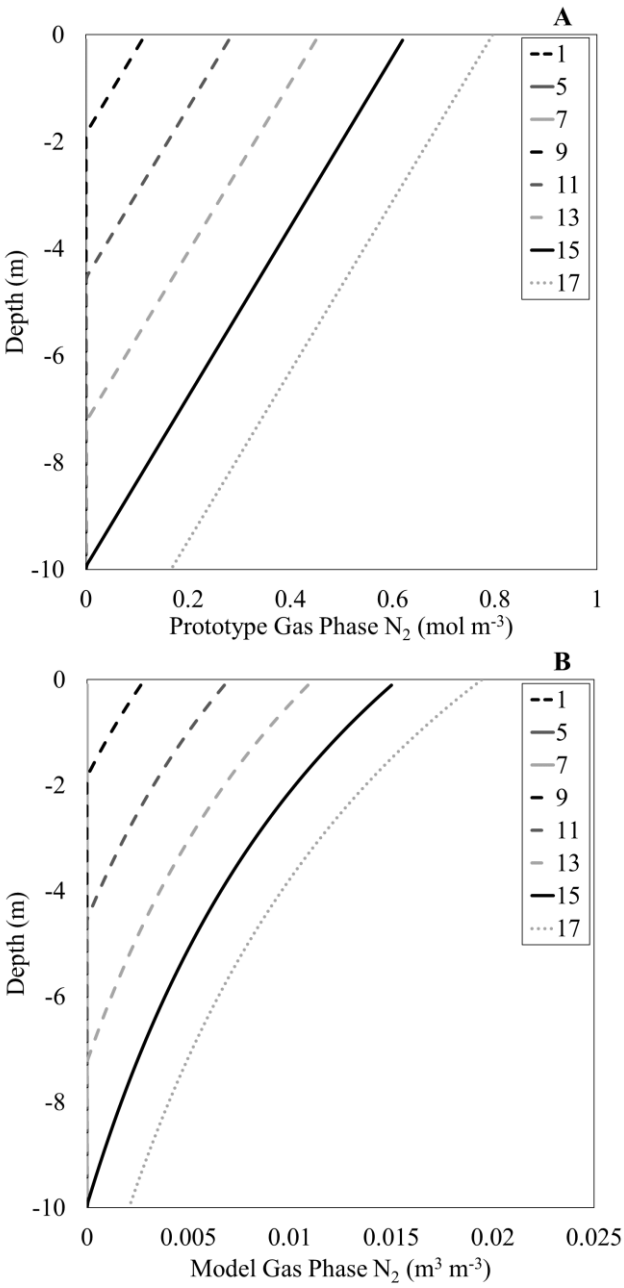

Figure 4. Gaseous $N_{2,(g)}$ ($N_{2(g),p}$) production over 17 hours at simulated prototype depth conditions at equilibrium considering biogenic N_2 production (r_{N2}), aqueous $N_{2,(aq)}$ diffusion between the layers ($J_{P,i}$ and $J_{P,i-1}$), and liquid-gas transfer ($c_{N2(g)}$) in Ottawa F-65 sand at 40% relative density by [A] mol and [B] volume.

4 CONCLUSIONS

Desaturation by biogenic gas production via denitrification has been proposed as a method for liquefaction mitigation. Preliminary lab-scale tests indicate that at shallow depth gas pockets may occur as a result of limited overburden pressure. Centrifuge tests can be performed to evaluate the performance of the process at field pressure conditions, prior to scale up to the field. As reactive transport processes scale differently with centrifuge-pressure conditions compared to the field it was expected the distribution in the centrifuge may differ from the expected distribution in the field. A simplified numerical model was developed and used to simulate the process at model and field scale. The results presented here indicate that diffusion of soluble $N_{2,(aq)}$ is negligible at both the model and prototype scales for the simulated reaction rate. Consequently, the change in saturation between model and field scale are similar, demonstrating that centrifuge testing has the potential to adequately simulate field conditions. However, the simplified model did not consider other pore scale influences, explicit consideration of the changes in permeability on gas stability, and mixing from liquid-gas transfer and transport. Future model enhancement to implement these features at continuum scale are recommended to improve understanding of biogenic gas behavior and its influence on the unsaturated soil mechanics .

5 ACKNOWLEDGEMENTS

Work described herein was supported by the National Science Foundation Geomechanics and Geosystems Engineering and Engineering Research Center programs under grants numbered CMMI-0703000, CMMI-0727463 CMMI-1233658, CMMI-0830182, and ERC-1449501. Operation of the centrifuge is supported by NSF under the NHERI program, CMMI-1520581. The authors are grateful for this support. Any opinions, findings and conclusions or recommendations expressed in this material are those of the authors and do not necessarily reflect those of the NSF.

6 REFERENCES

Cadogan, S.P., Maitland, G.C. & Trusler, J.P.M. 2014. Diffusion Coefficients of CO_2 and N_2 in Water at Temperatures between 298.15 K and 423.15 K at Pressures up to 45 MPa. *Journal of Chemical and Engineering Data*, 59: 519-525.

Caicedo, B. & Thorel, L. 2014. Centrifuge modelling of unsaturated soils. *Journal of Geo-Engineering Sciences*, 2: 83103.

Connolly, J.M., Jackson, B., Rothman, A.P., Klapper, I. & Gerlach, R. 2015. Estimation of a biofilm-specific reaction rate: kinetics of bacterial urea hydrolysis in a biofilm. *npjBiofilms and Microbiomes*, 1 (15014): 1-8.

DeJong, J.T., Mortensen, B.M., Martinez, B.C. & Nelson, D. C. 2010. Bio-mediated soil improvement. *Ecological Engineering*, *36*: 197–210.

Folger, H.S. 2005. *Essentials of Chemical Reaction Engineering*. 4th Ed., Prentice Hall.

Garnier, J., Gaudin, C., Springman, S.M., Culligan, P.J, Goodings, D., Konig, D., Kutter, B., Phillips, R., Randolph, M.F. & Thorel, L. 2007. Catalogue of scaling laws and similitude questions in geotechnical centrifuge modelling. *International Journal of Physical modelling in Geotechnics*, 3: 1-23.

He, J., Chu, J. & Ivanov, V. 2013. Mitigation of liquefaction of saturated sand using biogas. *Géotechnique*, 63(4): 267–275.

Kutter, B.L. 2012. Effects of capillary number, Bond number, and gas solubility on water saturation of sand specimens. *Canadian Geotechnical Journal*, 50: 133-144.

Neidhardt, F.C., Curtiss III, R., Ingraham, J.L., Lin, E.C.C., Low, K.B., Mgasanik, B., Reznikoff, W.S., Riley, M., Schaechter, M. & Umbarger, H.E. 1996. *Escherichia coli and Salmonella*. 2nd Edition, Volume 1. ASM Press, Washington, D.C.

O'Donnell, S. T., Kavazanjian, E., Jr. & Rittmann, B.E. 2017a. Liquefaction Mitigation via Microbial Denitrification as a Two-Stage Process, Stage I: Desaturation. Acccepted for publication, *Journal of Geotechnical and Geoenvironmental Engineering.*

O'Donnell, S. T., Kavazanjian, E., Jr. & Rittmann, B.E. 2017b. Liquefaction Mitigation via Microbial Denitrification as a Two-Stage Process, Stage II: MICP. Accepted for publication, *Journal of Geotechnical and Geoenvironmental Engineering*.

Pham, V., Nakano, A., Van der Star, W., Heimovaara, T. & van Paassen, L.A. 2016. Applying MICP by denitrification: A process analysis. *Environmental Geotechnics*.

Pham, V. 2017. *Bio-based Ground Improvement through Microbial Induced Desaturation and Precipitation (MIDP).* (Doctoral Dissertation). Delft University of Technology, Delft, The Netherlands.

Rebata-Landa, V. & Santamarina, J.C. 2012. Mechanical Effects of Biogenic Nitrogen Gas Bubbles in Soils. *Journal of Geotechnical and Geoenvironmental Engineering*, 138(2): 128 – 137.

Vaid, Y.P. & Sivathayalan, S. 2010. Fundamental factors affecting liquefaction susceptibility of sands. *Canadian Geotechnical Journal*, 37(3): 592 – 606.

van Paassen, L. A., Daza, C. M., Staal, M., Sorokin, D. Y., van der Zon, W. & van Loosdrecht, M. C. M. 2010. Potential soil reinforcement by biological denitrification. *Ecological Engineering*, 36: 168–175.